ARMY RESEARCH LABORATORY

Magnetic Signatures: Small Arms Testing of Multiple Examples of Same Model Weapons

by G. A. Fischer, J. E. Fine, and A. S. Edelstein

ARL-TR-4801 **April 2009**

NOTICES

Disclaimers

The findings in this report are not to be construed as an official Department of the Army position unless so designated by other authorized documents.

Citation of manufacturer's or trade names does not constitute an official endorsement or approval of the use thereof.

Destroy this report when it is no longer needed. Do not return it to the originator.

Army Research Laboratory
Adelphi, MD 20783-1197

ARL-TR-4801 **April 2009**

Magnetic Signatures: Small Arms Testing of Multiple Examples of Same Model Weapons

G. A. Fischer, J. E. Fine, and A. S. Edelstein
Sensors and Electron Devices Directorate, ARL

REPORT DOCUMENTATION PAGE	Form Approved OMB No. 0704-0188

1. REPORT DATE *(DD-MM-YYYY)*	2. REPORT TYPE	3. DATES COVERED (From - To)
April 2009	Final	October 2006 to March 2007

4. TITLE AND SUBTITLE

Magnetic Signature: Small Arms Testing of Multiple Examples of Same Model Weapons

5a. CONTRACT NUMBER

5b. GRANT NUMBER

5c. PROGRAM ELEMENT NUMBER

6. AUTHOR(S)

G. A. Fischer, J. E. Fine, and A. S. Edelstein

5d. PROJECT NUMBER

5e. TASK NUMBER

5f. WORK UNIT NUMBER

7. PERFORMING ORGANIZATION NAME(S) AND ADDRESS(ES)

U.S. Army Research Laboratory
ATTN: AMSRD-ARL-SE-SP
2800 Powder Mill Road
Adelphi, MD 20783-1197

8. PERFORMING ORGANIZATION REPORT NUMBER

ARL-TR-4801

9. SPONSORING/MONITORING AGENCY NAME(S) AND ADDRESS(ES)

10. SPONSOR/MONITOR'S ACRONYM(S)

11. SPONSOR/MONITOR'S REPORT NUMBER(S)

12. DISTRIBUTION/AVAILABILITY STATEMENT

Approved for public release; distribution unlimited.

13. SUPPLEMENTARY NOTES

14. ABSTRACT

This report investigates identical model small arms, in particular eight same-model pistols and seven same-model shotguns. This is an adjunct to experiments to obtain statistically significant quantities of signatures of objects of military interest. Magnetic signature features were compared to find similarities and differences between all the pistols and all the shotguns tested. In the far field region, the shapes of the component curves for each weapon were similar; the relative shapes of the component signals, however, were different for both types of weapon. A comparison of total field decay with distance from pistol to sensor showed a noticeable difference when the experiment was performed indoors when compared with an open field. Finite element simulations were done to demonstrate the effect of nearby ferrous objects on the total field decay with distance.

15. SUBJECT TERMS

Magnetic signatures, small arms, weapons, magnetic modeling

16. SECURITY CLASSIFICATION OF:			17. LIMITATION OF ABSTRACT	18. NUMBER OF PAGES	19a. NAME OF RESPONSIBLE PERSON
a. REPORT	b. ABSTRACT	c. THIS PAGE	UU	26	G. A. Fischer
Unclassified	Unclassified	Unclassified			19b. TELEPHONE NUMBER (*Include area code*) (301) 394-2089

Contents

List of Figures

Executive Summary

This report investigates identical model small arms, in particular eight same-model pistols and seven same-model shotguns. This is an adjunct to experiments to obtain statistically significant quantities of signatures of objects of military interest. Studies of several copies of two kinds of tanks were presented in a recent paper (*1*). Data was obtained with two Model DFM100G2 Billingsley three-axis fluxgate magnetometers in a building at the U.S. Army Research Laboratory (ARL) Adelphi Center. These magnetometers were sampled at 43 Hz. The test grid consisted of a series of intersecting North-South and East-West paths spaced at one-foot intervals. One magnetometer was placed within the test grid and the other was placed about 30 ft from the grid to simultaneously obtain data for background subtraction. In one series of tests, each weapon was carried in a single direction at increasing distances from the sensor to determine the far field distance threshold. The distances required to be in the far field were 3 ft and 5 ft for the pistols and shotguns, respectively. In another series of tests, each weapon was carried along the sets of intersecting paths in the far field of the grid sensor. These tests were done for a vertical and a horizontal muzzle orientation of each weapon and were used to calculate the magnetic moments of each weapon.

Magnetic signature features were compared to find similarities and differences between all the pistols and all the shotguns tested. The values for the total field for pistols carried in the North-South direction at a distance of 3 ft from the sensor are shown in figure 1. In the far field region, the shapes of the component curves for each weapon were similar. However, the relative shapes of the component signals were different for both types of weapons. The total field of the pistols in some cases was larger than the shotguns when both weapons were oriented vertically.

A comparison of total field decay with distance from pistol to sensor showed a noticeable difference when the experiment was performed indoors when compared with an open field (figure 2). Outside the amplitude decreased as $1/r^3$, as expected. The signal decreased much more rapidly inside the building, possibly caused by the presence of steel columns or steel reinforcement bars in the floor, or ferrous metal elsewhere in the building. Finite element simulations were done to demonstrate the effect of nearby ferrous objects on the total field decay with distance.

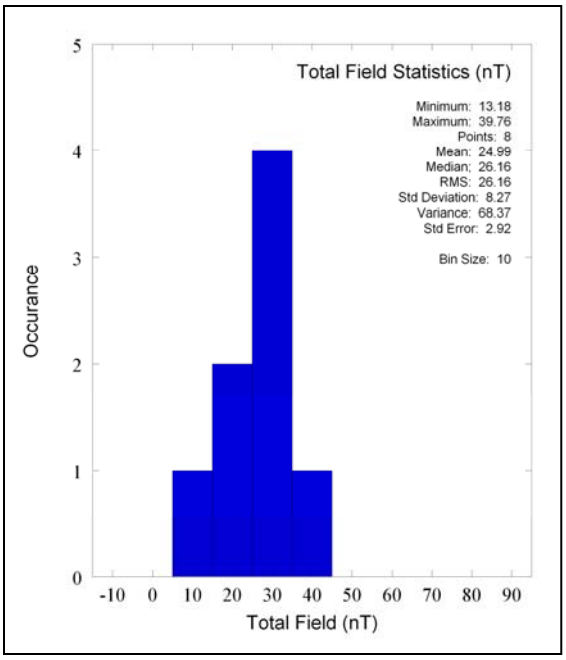

Figure 1. Distribution of magnetic total field values for eight identical pistols, orientation 1, ~3.60 ft from sensor, walking from north to south.

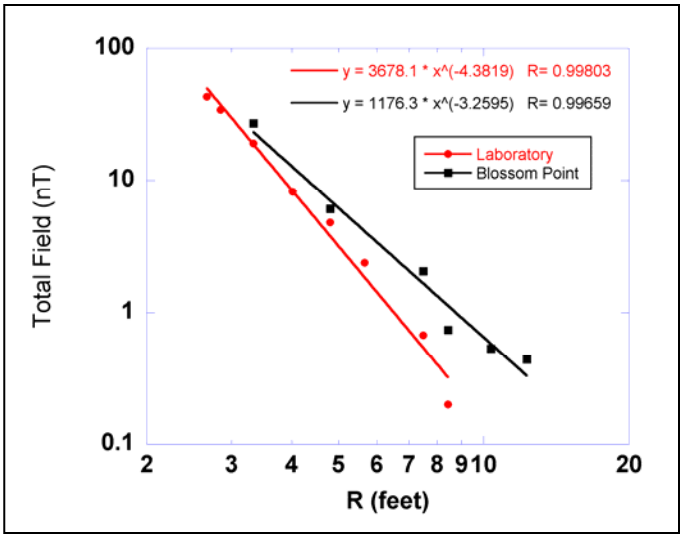

Figure 2. Total field values for a pistol, orientation 1, indoors and outside.

1. Introduction

The magnetics program at the U.S. Army Research Laboratory (ARL) is primarily directed at exploring and supporting the use of magnetic sensors for Army applications. To that end, the ARL magnetics group actively works on the evaluation of currently available sensors and sensor systems, the development of sensors and sensor systems, cataloging and evaluating magnetic signatures, algorithm development, and demonstrations of magnetic sensor utility. The pursuit of these activities entails not only an onsite research program, but also maintaining awareness of current magnetic technology, providing research support, and collaborating with other labs. This is part of the Unattended Ground Sensors (UGS) program, which has the goal of scattering many low-cost, low-power sensors of various modalities on the battlefield to locate, identify, and track targets of military interest.

Magnetic sensors are useful for military sensing because it is difficult and expensive to design weapons and weapon systems without including some ferromagnetic material. Though magnetic sensors have limited range, they offer the advantages of insensitivity to weather conditions, require only a small amount of bandwidth, and have the ability to sense through foliage. A recent report has discussed the range of vehicles and a rifle detectable by a magnetometer (*2*). This report focuses on detection of small arms by magnetic sensors. In this report, we focus on our tests using pistols, shotguns, and previously obtained AK47 data. This will, hopefully, lead to the use of magnetic sensors as a "trip-wire" detector for perimeter protection, and as a weapons detector to enhance airport security.

This investigation employed a rectangular grid course adapted from the intersecting magnetic north-south/east-west path method used in a recent test at Eglin Air Force Base (AFB), FL (*3*). The objectives of our test were to (1) determine variability of the weapon's total field values, (2) estimate the detection range of the weapon using conventional laboratory magnetometers, and (3) analyze the magnetic component wave forms obtained. This report contains the results of a completed aspect of a larger effort.

2. Experimental Details

The experiments we will be discussing were conducted indoors at ARL in Adelphi (Bldg. 507), as well as outdoors at the Aberdeen Proving Ground (APG) and at ARL's Blossom Point testing range. The indoors segment of the testing was conducted inside a largely wooden construction building that houses the magnetics team testing facility. We have shown previously (*2*) that intersecting north-south and east-west paths, in conjunction with a single three-axis magnetometer, can be used to determine the magnetic moment magnitude of vehicles, such as a

tank, truck, and a High Mobility Multipurpose Wheeled Vehicle (HMMWV). A similar grid was adapted for use in these tests. An example is shown in figure 3. A similar arrangement was used for the outside tests, but the instrumentation system was at least 30 ft away, and there were no ferrous objects, such as metal furniture or steel support posts, present. Experiments with pistols involved three different orientations of the pistol, while those involving the shotguns used two different orientations of the weapon.

Figure 3. Test arrangement for small arms inside the wooden building, showing a three-axis fluxgate magnetometer, north-south path lines, and instrumentation system.

Two different types of vector magnetometers were used in these tests. In some instances the FVM-400 Vector Fluxgate Magnetometer by Macintyre Electronics Design Associates, Inc. (MEDA) was used and in other cases two DFM100G2 Digital Fluxgate Magnetometers made by Billingsley Magnetics were used. The majority of the data obtained was done with the latter. The MEDA has a 1 nT resolution, while the Billingsley magnetometer has an ultimate resolution of 0.1 to 0.2 nT. In the case of the Billingsley magnetometers, one magnetometer was used as reference so a gradiometer approach could be employed to extend detection range.

Magnetic field components were acquired for each run of each weapon and examined to make qualitative statements concerning variability amongst identical weapon types and differences between weapons. Detection range data points for the weapons were determined by calculating the total field for each run and then plotting versus distance. The total field amplitude (B_{TOT}) is simply

$$B_{TOT} = \sqrt{B_x^2 + B_y^2 + Bz^2} \quad (1)$$

where B_x, B_y, and B_z are the vector field components. The distance of the weapon from the sensor at the point of closest approach to the sensor of the person carrying the weapon is determined from

$$D = \sqrt{PCA^2 + h^2} \tag{2}$$

Where D is the distance of the weapon from the sensor, PCA is at the point of closest approach to the sensor by the person carrying the weapon, and h is the distance of the center point of the weapon above the ground (figure 4).

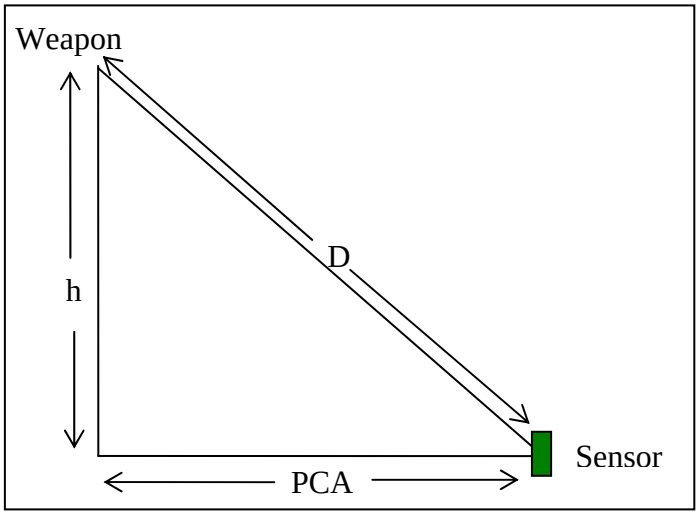

Figure 4. Diagram illustrating determination of weapon distance from sensor.

Simple magnetic models were run using a finite element code called Maxwell 3D, from Ansoft Corp. The geometry of the objects to be modeled is defined, properties are assigned to each object, seeding and meshing are performed, and then the 3D DC magnetic solver accurately computes static magnetic fields. These models are then used to discuss the fits to the range data obtained.

3. Results and Discussion

3.1 Qualitative Magnetic Vector Field Component Analysis

The *x*-, *y*-, and *z*-magnetic field component waveform shapes contain information about differences between weapons, orientations, and directions of movement. In gathering this data, we have attempted to stay in the far field of the device, usually one or two times its longest dimension. Most targets in this region have lost their primary distinguishing waveform features,

and appear like a magnetic dipole. The differences in the waveforms of visually identical targets may be attributed to differences in permanent and induced dipole moments, which cause variations in the orientation of the total or net moment.

Qualitative analysis of the vector components yielded a significant degree of uniformity within a given weapon type, holding weapon orientation, distance, and direction constant. For the purposes of illustration, we shall focus on pistols at a PCA of 1 ft that were carried in what we refer to as orientation 1 (figure 5). In figures 6 and 7 we show typical magnetic vector field components obtained for pistols traveling along North to South and East to West paths. Note that for both sets of paths, there is a reversal in the occurrence in time of the minimum of one of the components. In the case of the north to south sets, this occurs in the *x*-component, while for the case of the east to west sets this occurs in the *y*-component.

Figure 5. Orientation “1” for pistol testing.

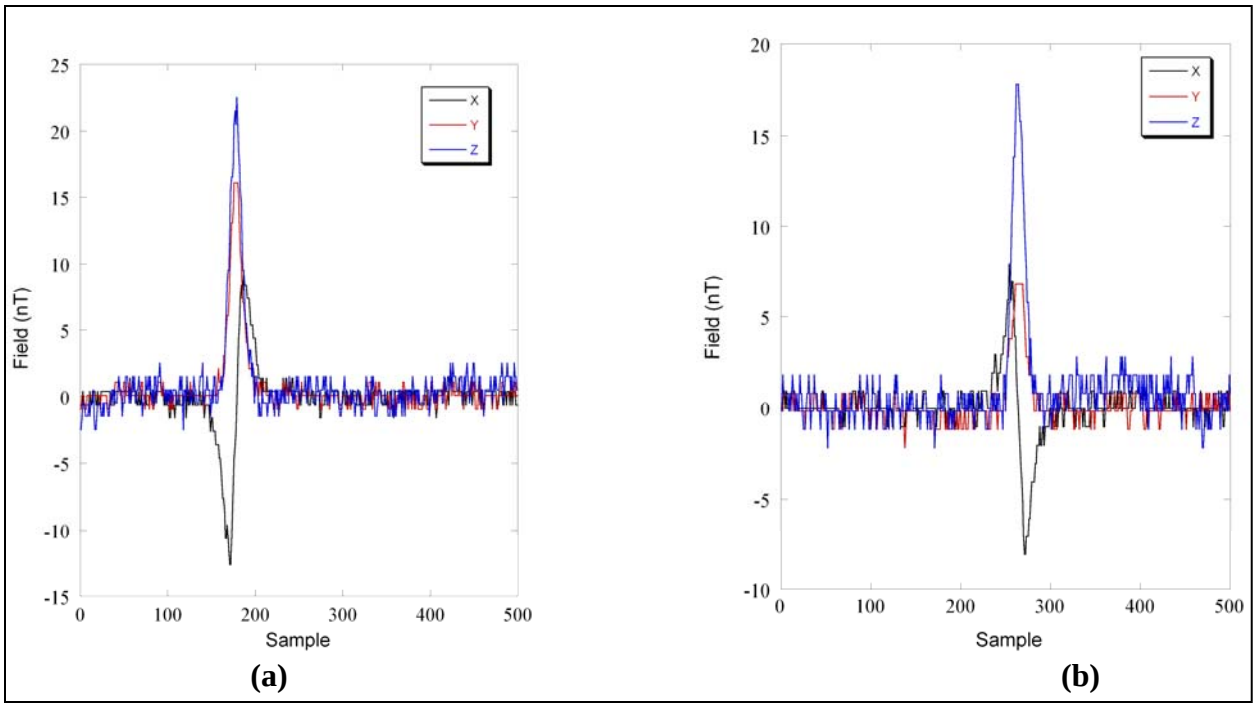

Figure 6. Typical magnetic vector field components for a pistol in orientation 1, PCA of 1 ft, when traveling from (a) north to south and (b) south to north

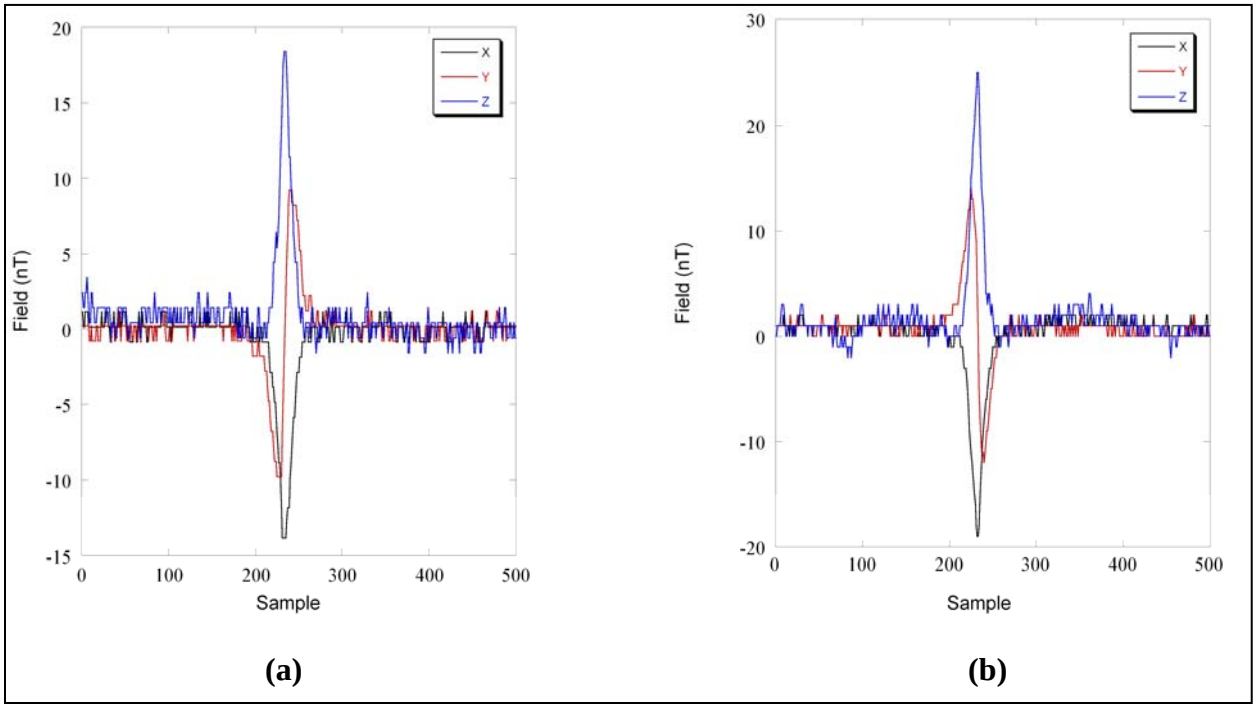

Figure 7. Typical magnetic vector field components for a pistol in orientation 1, PCA of 1 ft, when traveling from (a) east to west and (b) west to east.

In figures 8 and 9 we show the magnetic field components typical of shotguns at a PCA of 5 ft from the sensor and carried on one's shoulder. Comparing these component shapes and behaviors to those of the shotguns indicates that there are discernable differences. We again note that for both sets of paths there is a reversal in the occurrence in time of the minimum of one of the components. In the case of the north to south sets, this again occurs in the *x*-component, while for the case of the east to west sets this occurs in the *y*-component. However, in the case of the shotguns, there is an additional change in the case of the shotgun that does not occur for pistols. We note that the *z*-component also changes with a change in direction of motion.

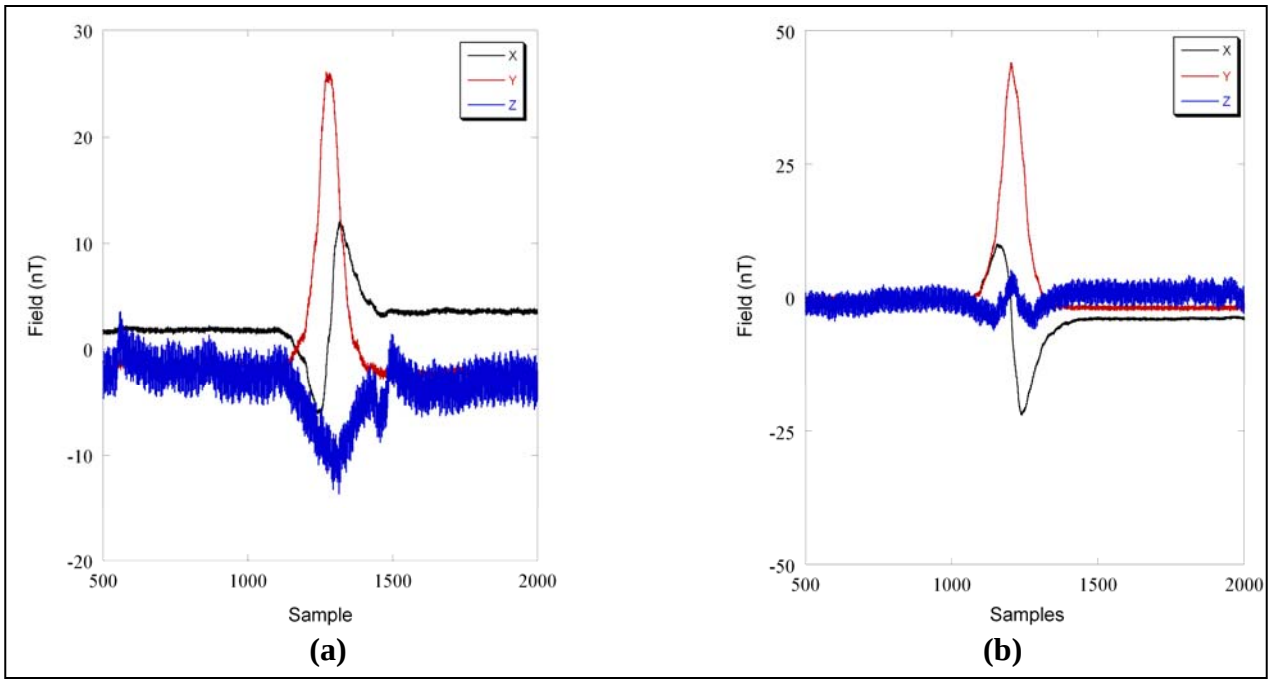

Figure 8. Typical magnetic vector field components for a shotgun carried on the shoulder, PCA of 5 ft, when traveling from (a) north to south and (b) south to north.

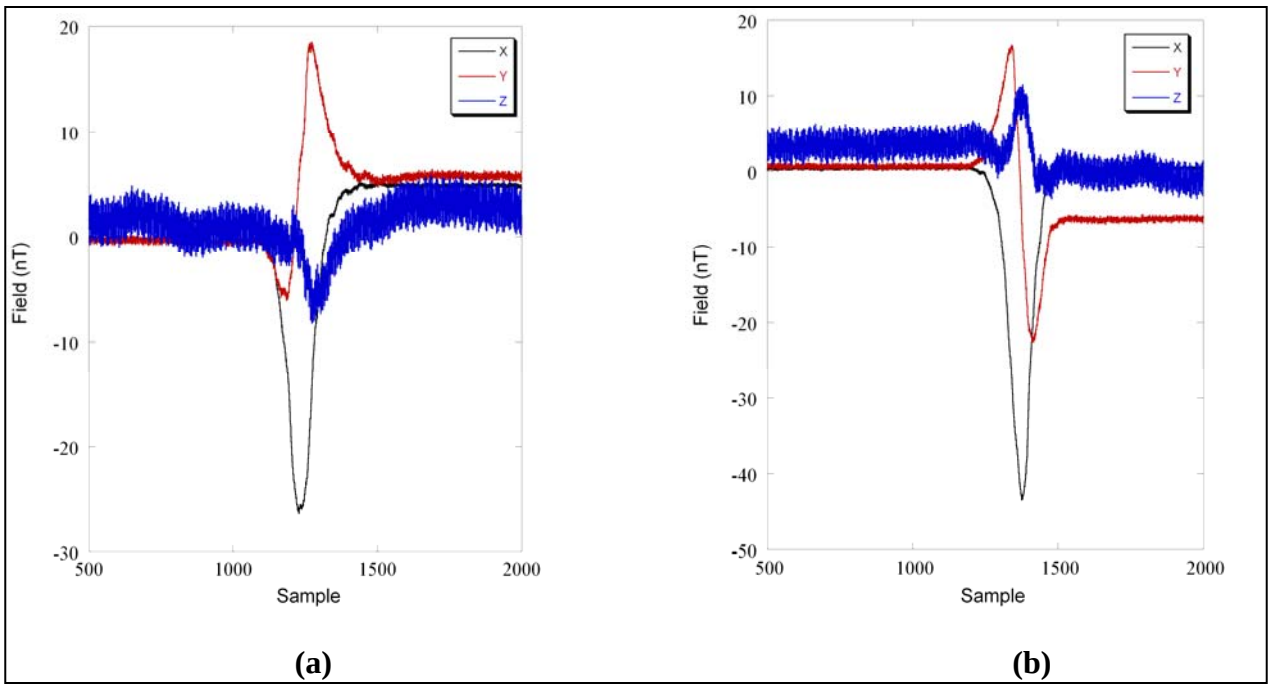

Figure 9. Typical magnetic vector field components for a shotgun carried on the shoulder, PCA of 5 ft, when traveling from (a) east to west and (b) west to east.

3.2 Total Field Statistics and Detection Range Determination

If one is to make any statements about classification or identification of objects of interest using magnetic signature data, one must first make sure that same-type objects yield identical signatures when acquired under identical circumstances (i.e., alignment of sensor, direction of travel of object, etc.). To that end we analyzed variations in the total field values obtained from our experiments with eight pistols. These values, as shown in figure 1, do tend to group together; however, we note that while graphical depictions of the distribution indicated a grouping of the values, the standard deviation is typically ~30% of the mean. It is rather surprising that a variation exists amongst supposedly identical weapons.

For the purposes of this report we will again focus on orientation 1 for the pistols with a PCA of 1 ft. Part of this analysis involved dealing with small signals relative to the ambient background, noisy backgrounds, and thermal drift in the sensors in the case of testing outdoors. While one cannot assume identical thermal drift properties between sensors, the use of two sensors helped with these issues. One sensor is used to detect the object of interest, while the other is located at a distance sufficient to not avoid detecting the object. Data is collected from both sensors simultaneously on the same computer. A fit is made to the thermal drift in the data of each sensor and then subtracted. Next, the ambient background data is subtracted from the data containing the signal of interest. Finally, if necessary, the signal is smoothed by averaging over

five data points at a time in an effort to discern details. This processing is illustrated in figure 10. The amplitude of the total field should decrease with increasing distance from the sensor as $1/r^3$, where r is the distance.

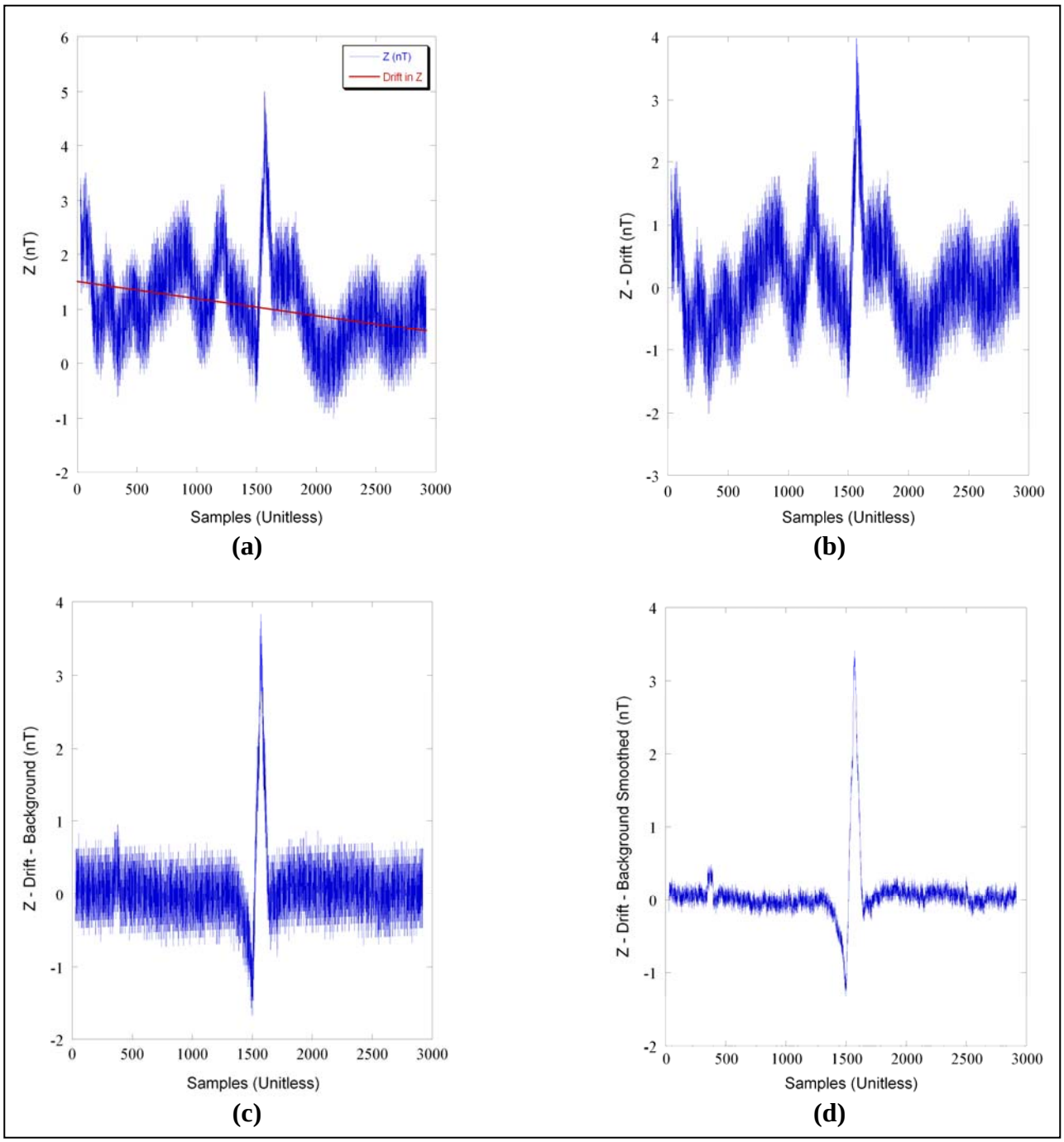

Figure 10. Illustration of our data processing steps. A fit is made to the thermal drift of both (only shown for one) sensors (a), the drift is subtracted from both sensors (b), the ambient background sensor data is then subtracted from the signal (c), and finally the signature is smoothed. The two Billingsley magnetometers are used for these measurements and analysis steps.

As we saw in figure 2, the fit to the total field data obtained in the wooden building for range determination of a pistol yielded $1/r^{4.4}$. We took the same pistol that we used for this data to ARL's Blossom Point testing range to repeat the experiment and we see that there the fit yields a value of $1/r^{3.3}$. This is not the first time we have arrived at total field values that do not fall off as $1/r^3$. Figure 11 shows total field values versus distance for an AK47 having a wooden stock that were obtained in a test at APG. The detection range of the AK47 is compared to that of the pistol obtained at Blossom Point. The lines in figure 11 are what a $1/r^3$ behavior would have been for both weapons. Deviations from $1/r^3$ will be discussed further in section 3.3 of this report.

In the case of the AK47, we should note that the weapons are made from many designs which depend on country of origin and manufacturer. Therefore, we may expect variations from one type to another. Figure 11 shows that for the fluxgate magnetometer used, which has a sensitivity of 0.2 nT, one can detect the pistol to about 12 ft, and the AK47 to about 14 ft. If technological improvements, such as ARL's MEMs Flux Concentrator (*4*), can be made to AMR magnetometers that have a sensitivity of 7 nT to extend the sensitivity to 0.01 nT, the pistol might be detected at 42 ft and the AK47 at 62 ft.

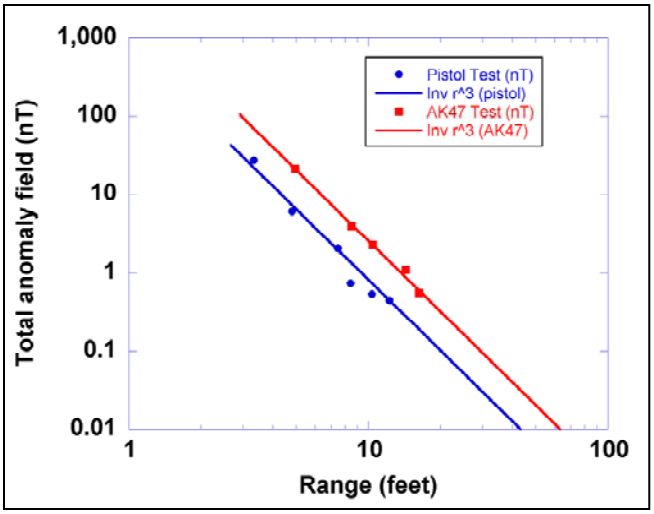

Figure 11. A comparison of detection ranges of a pistol and an AK47, both tested in the field.

Note: Solid lines indicate how a $1/r^3$ behavior would compare to the data.

3.3 Magnetic Modeling and the Effect of Nearby Ferrous Objects on the Total Field Values

As mentioned in section 3.2, we have, on more than one occasion, observed total field values that do not fall off as $1/r^3$. We feel this is due to the presence of ferrous materials in the test area that are not only distorting the Earth's magnetic field, but also the field of the object of interest. To demonstrate that this can result in the power laws we have observed, simple magnetic models were run using a finite element code called Maxwell 3D, from Ansoft Corp. As this is a static

modeling program, we relied on the fact that a ferromagnetic object moving past a stationary sensor at a given distance will produce, holding all other parameters constant, a response indistinguishable from that of a sensor moving past a stationary ferromagnetic object.

A permanent magnet was used in the model as the object of interest. The magnet is a short cylinder, or disk shaped (figure 12). Data was extracted from the finished model along the center (*y*-axis) axis of the cylinder. Extracting data in this manner is analogous to the case of a stationary magnet and a sensor acquiring data as it moves away from the magnet along a line parallel to the magnet's center axis. By symmetry, this is in turn analogous to a stationary sensor acquiring data while a magnet moves away from it along this path.

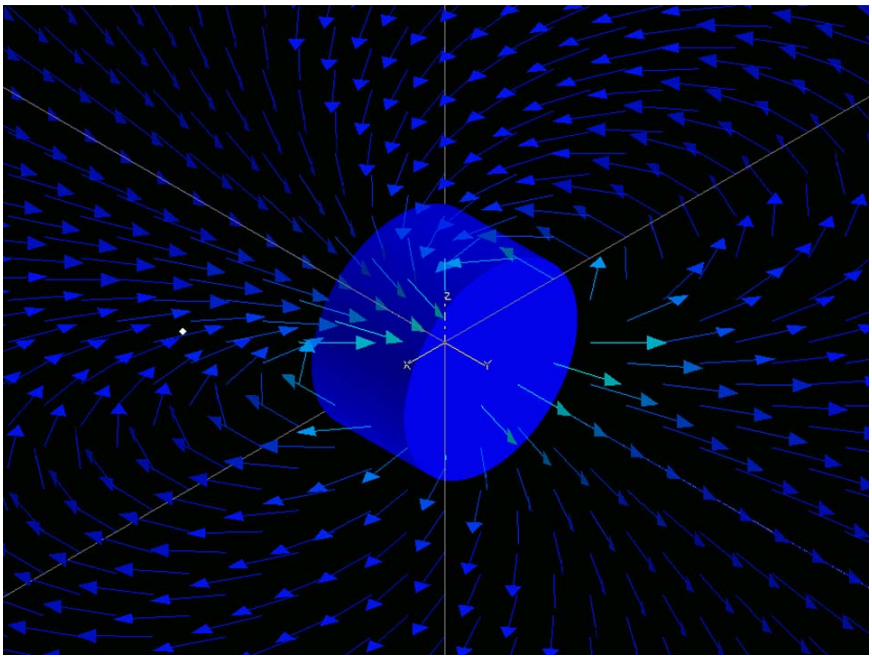

Figure 12. The disk shaped magnet and the B-field in the *xy* plane.

Note: The *z*-axis is vertical in the image while the *y*-axis is at the center of the face of the magnet.

The model was run under three different circumstances. First, only the magnet and its field were present. This was done to demonstrate the model works and that a $1/r^3$ relationship results from the data. Next, the model was run again with a uniform external field applied that is approximately equal to that of the Earth's field, 0.53 Oe. Finally, an additional object was added to the model in the form of a long rod (figure 13) of first (a) 1040 steel and then simply a high permeability material. In the latter case, the permeability assigned to the material was 500.

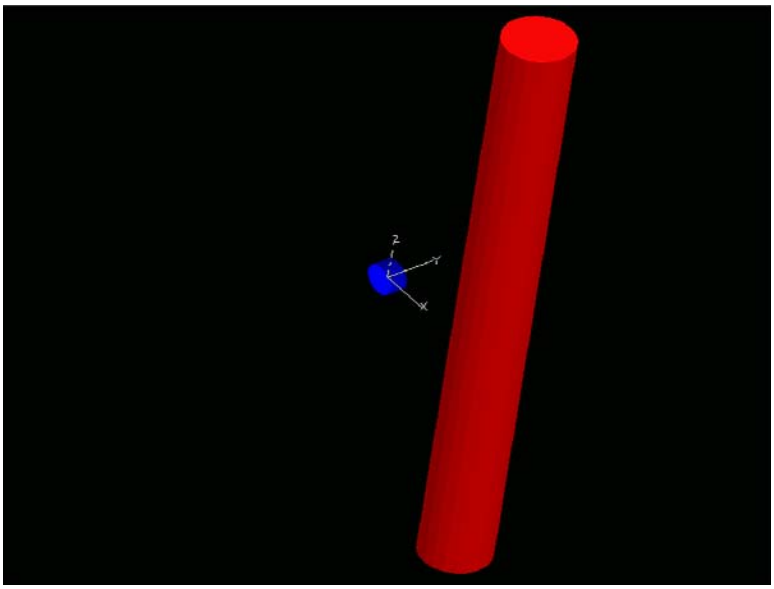

Figure 13. Placement of 20 cm long rod with radius of 1 cm, relative to magnet. Magnet has radius of 0.5 cm and height of 0.5 cm. Center of rod is 3 cm away from the magnet.

In figure 14 we see that the magnet by itself does essentially yield a $1/r^3$ relationship. Adding the Earth's field alters the fit slightly, more than likely due to the influence of the Earth's flux lines on those of the magnet. For both the 1040 steel pole and the permeable material pole, we see significant deviations the $1/r^3$ relationship. The result of the model for the permeable material rod is shown in figure 15; note that the result is close to that observed at Blossom Point. We believe that deviations from the $1/r^3$ relationship typically are due to the influence of other materials in the surrounding environment.

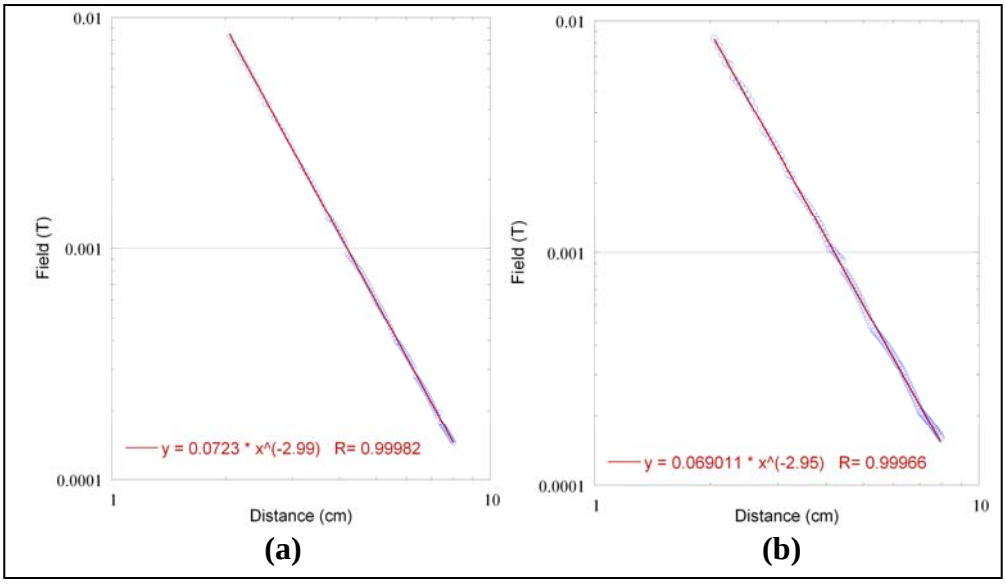

Figure 14. Variation of total magnetic field values with distance for (a) a hard magnet and (b) for a hard magnet immersed in the Earth's field.

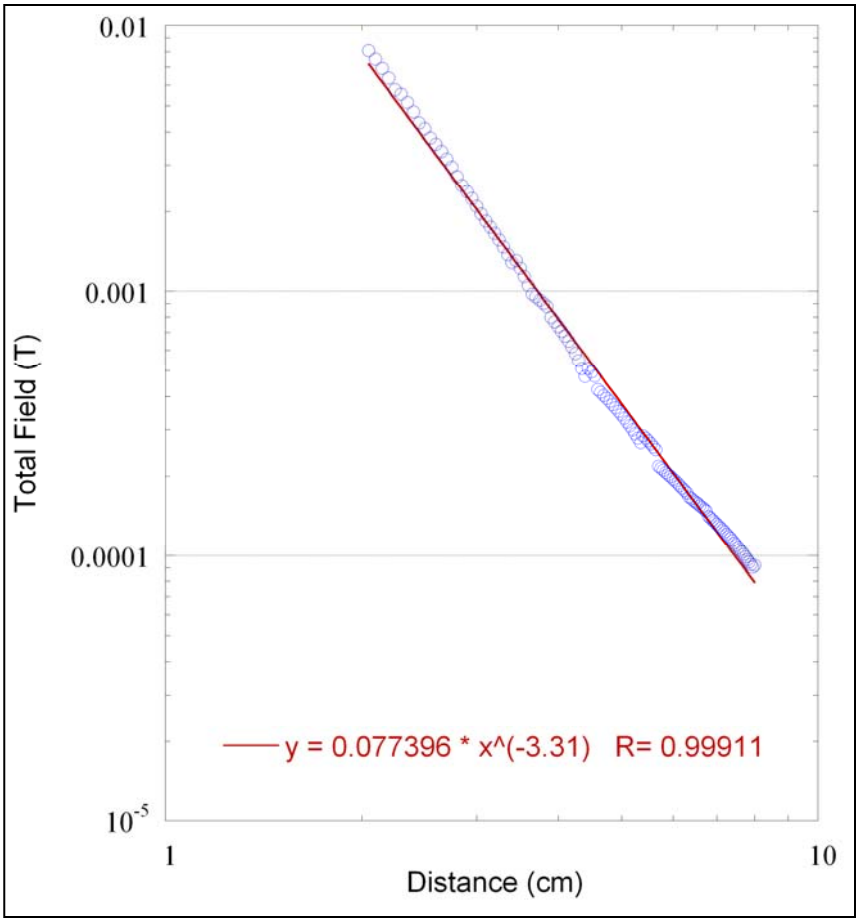

Figure 15. Variation of total magnetic field values with distance for a hard magnet, immersed in the Earth's field, with a permeable object near by.

4. Conclusions

Using two different types of fluxgate vector magnetometers, we have obtained the signatures of eight same-model pistols and seven same-model shotguns. In some instances this data was compared to that obtained previously of an AK47. Even though we focused on data for when the weapons were in the far field, qualitative statements could be made illustrating how the signatures of the shotguns differ from those of the pistols. Comparing the component shapes and behaviors to those of the shotguns indicated that there are discernable differences in magnitudes and shapes of the curves, as well as a difference in how signatures changed when the direction of travel was changed. Specifically, the *z*-component also changes with a change in direction of motion for shotguns. This does not occur with the pistols. Analyses of the distribution of total field values for the pistols were examined to determine if there is a large variation amongst supposedly identical weapons. We showed the standard deviation is about 30% of the mean value for the pistols. The variations of the total magnetic field of the pistols with distance were

determined both indoors and outside at a test range. In both instances, fits to the data did not yield the expected $1/r^3$ relationship. Magnetic modeling was used to demonstrate that this is probably due to the presence of ferrous materials in the surrounding environment. This small arms analysis will be extended to complete the analysis and comparison of the shotguns to the pistols. The ultimate goal of that study will be to make a statement regarding the possibility of distinguishing between pistols and shotguns.

5. References

1. Fischer, G. A.; Fine, J. E.; Edelstein, A. S. Advances in Magnetic Signature Identification (U). *IRIA/MSS Proceedings 2004 Meeting of the MSS Specialty Group on Battlefield Acoustic and Magnetic Sensing (U)*, Volume II, December 2004. Johns Hopkins University, Applied Physics Laboratory, Laurel, MD, 23–24 August 2004.

2. Fischer, G. A.; Fine, J. E.; Edelstein, A. S. Aberdeen Magnetics Field Test. *Battlefield Acoustic & Seismic Sensing, Magnetic & Electric Field Sensors Military Sensing Symposium*, Johns Hopkins University, Applied Physics Laboratory, Laurel, MD, 23–26 September 2002.

3. Fine, J. E. Magnetic Measurements of Military Vehicles at Eglin AFB. *Battlefield Acoustic & Seismic Sensing, Magnetic & Electric Field Sensors Military Sensing Symposium, ,* Johns Hopkins University, Applied Physics Laboratory, Laurel, MD, 7–10 October 2003.

4. Edelstein, A.; Fischer, G., U.S. Army Research Laboratory, Adelphi, MD; Pedersen, M., MEMS Exchange, Reston, VA; Cheng, S. F., Naval Research Laboratory, Washington, D.C. Development of a MEMS Flux Concentrator Magnetometer. E.3. *2005 Meeting of the Military Sensing Symposia (MSS) Specialty Group on Battlefield Acoustic & Seismic Sensing, Magnetic & Electric Field Sensors*, Johns Hopkins University, Applied Physics Laboratory, Laurel, MD, 23–25 August 2005.

List of Symbols, Abbreviations, and Acronyms

AFB	Air Force Base
APG	Aberdeen Proving Ground
ARL	U.S. Army Research Laboratory
HMMWV	High Mobility Multipurpose Wheeled Vehicle
MEDA	Macintyre Electronics Design Associates
UGS	Unattended Ground Sensor

NO. OF COPIES	ORGANIZATION
1	ADMNSTR
ELECT	DEFNS TECHL INFO CTR ATTN DTIC OCP 8725 JOHN J KINGMAN RD STE 0944 FT BELVOIR VA 22060-6218
1	DARPA ATTN IXO S WELBY 3701 N FAIRFAX DR ARLINGTON VA 22203-1714
1	DEFNS INTLLGNC AGCY ATTN RTS-2A TECHL LIB WASHINGTON DC 20301
1 CD	OFC OF THE SECY OF DEFNS ATTN ODDRE (R&AT) THE PENTAGON WASHINGTON DC 20301-3080
1	US ARMY RSRCH DEV AND ENGRG CMND ARMAMENT RSRCH DEV AND ENGRG CTR ARMAMENT ENGRG AND TECHNLGY CTR ATTN AMSRD AAR AEF T J MATTS BLDG 305 ABERDEEN PROVING GROUND MD 21005-5001
1	US ARDEC ATTN AMSRD AAR HEP A M HOHIL BLDG 407 PICATINNY ARSENAL NJ 07806-5000
1	US ARMY ARDEC ATTN AMSRD AAR AEP S R T KINASEWITZ BLDG 353N PICATINNY ARSENAL NJ 07806-5000
1	US ARMY ARDEC ATTN AMSRD AAR EMK TECH LIB BLDG 59 PHIPPS RD PICATINNY ARSENAL NJ 07806-5000
1	US ARMY INFO SYS ENGRG CMND ATTN AMSEL IE TD F JENIA FT HUACHUCA AZ 85613-5300

NO. OF COPIES	ORGANIZATION
1	COMMANDER US ARMY RDECOM ATTN AMSRD AMR W C MCCORKLE 5400 FOWLER RD REDSTONE ARSENAL AL 35898-5000
1	NAV RSRCH LAB ATTN 5220 TECHL LIB 4555 OVERLOOK AVE SW WASHINGTON DC 20375-5320
1	US GOVERNMENT PRINT OFF DEPOSITORY RECEIVING SECTION ATTN MAIL STOP IDAD J TATE 732 NORTH CAPITOL ST NW WASHINGTON DC 20402
1	THE JOHNS HOPKINS UNIV APPLD PHYSIC LAB ATTN TECH LIB JOHNS HOPKINS RD LAUREL MD 20707
1	ANSOFT CORP. FOUR STATION SQUARE, SUITE 200 PITTSBURGH PA 15219-1119
1	SOUTHWEST RSRCH INST ATTN S CERWIN 6220 CALEBRA RD SAN ANTONIO TX 78238
1	SSP ATTN C GAILBREATH ASSOC TECHL DIR ATTN T HAWLEY TECHL DIR 11781 LEE JACKSON MEMORIAL HWY FAIRFAX VA 22033-3309
1	US ARMY RSRCH LAB ATTN AMSRD ARL CI OK TP TECHL LIB T LANDFRIED BLDG 4600 ABERDEEN PROVING GROUND MD 21005-5066

NO. OF COPIES	ORGANIZATION
1	DIRECTOR US ARMY RSRCH LAB ATTN AMSRD ARL RO EV W D BACH PO BOX 12211 RESEARCH TRIANGLE PARK NC 27709
20	US ARMY RSRCH LAB ATTN AMSRD ARL CI OK PE TECHL PUB ATTN AMSRD ARL CI OK TL TECHL LIB ATTN AMSRD ARL SE J PELLEGRINO ATTN AMSRD ARL SE S J EICKE ATTN AMSRD ARL SE S R SARTAIN ATTN AMSRD ARL SE SP A EDELSTEIN ATTN AMSRD ARL SE SP M SCANLON ATTN AMSRD ARL SE SS A LADAS ATTN AMSRD-ARL-SE-SP G FISCHER (10 COPIES) ATTN AMSRD-ARL-SE-SP J FINE ATTN IMNE ALC HRR MAIL & RECORDS MGMT ADELPHI MD 20783-1197
TOTAL:	38 (36 HCS, 1 CD, 1 ELECT)

INTENTIONALLY LEFT BLANK